

SPIN RESPONSE OF THE NUCLEON IN THE RESONANCE REGION*

VOLKER D. BURKERT

*Jefferson Lab, 12000 Jefferson Avenue
Newport News, Virginia 23606, USA*

Abstract

I discuss recent results from CLAS and Hall A at Jefferson Lab on the measurement of inclusive spin structure functions in the nucleon resonance region using polarized electron beams and polarized targets. Results on the first moment of the spin structure function for protons and neutrons will be discussed, as well as the Bjorken integral. I will argue that the helicity structure of individual resonances plays a vital role in understanding the nucleon's spin response in the domain of strong interaction QCD, and must be considered in any analysis of the nucleon spin structure at low and intermediate photon virtuality.

1. Introduction

For more than 20 years, measurements of polarized structure functions in lepton nucleon scattering have been a focus of nucleon structure physics at high energy laboratories. One of the surprising findings of the EMC experiment at CERN was that only a small fraction of the nucleon spin is accounted for by the spin of the quarks¹. The initial results were confirmed by several follow-up experiments². This result is in conflict with simple quark model expectations, and demonstrated that we are far from having a realistic picture of the nucleon's internal structure. These experiments also studied the fundamental Bjorken sum rule³ which, at asymptotic momentum transfer, relates the proton-neutron difference of the first moment $\Gamma_1 = \int g_1(x)dx$ to the weak axial coupling constant: $\Gamma_1^p - \Gamma_1^n = \frac{1}{6}g_A$. This sum rule has been evolved to the finite Q^2 values reached in the experiments using pQCD, and has been verified at the 5% level.

While these measurements were carried out in the deep inelastic regime, the nucleon's spin response has hardly been measured in the low Q^2 regime and in the domain of nucleon resonances, which is the true domain of strong QCD. Our understanding of nucleon structure is incomplete, at best, if the nucleon is not also

*Talk presented at the Second Asia Pacific Conference on Few Body Problems in Physics, Shanghai, China, August 27 - 30, 2002

probed and fundamentally described at medium and large distance scales. This is the domain where current experiments at JLab have their greatest impact.

While the Bjorken sum rule provides a fundamental constraint at large Q^2 , the Gerasimov-Drell-Hearn (GDH) sum rule ^{4,5} constrains the evolution at very low Q^2 . The GDH sum rule relates the differences in the helicity-dependent total photoabsorption cross sections to the anomalous magnetic moment κ of the target

$$\frac{M^2}{8\pi^2\alpha} \int_{\nu_0}^{\infty} \frac{\sigma_{1/2}(\nu) - \sigma_{3/2}(\nu)}{\nu} d\nu = -\frac{1}{4}\kappa^2 \quad (1)$$

where ν_0 is the photon energy at pion threshold, and M is the nucleon mass. The GDH sum rule also defines the slope of $\Gamma_1(Q^2 = 0)$, where the elastic contribution at $x = 1$ has been excluded:

$$2M^2 \frac{d\Gamma_1}{dQ^2}(Q^2 \rightarrow 0) = -\frac{1}{4}\kappa^2 \quad (2)$$

The sum rule has been studied for photon energies up to 2.5 GeV ⁶, and in this limited energy range deviates from the theoretical asymptotic value by less than 10%. A rigorous extension of the sum rule to finite Q^2 has been introduced by Ji and Osborne ⁷. Measurement of the Q^2 -dependence of (1) allows tests of the low energy QCD predictions of the GDH sum rule evolution in ChPT, and shed light on the question at what distance scale pQCD corrections and the QCD twist expansion will break down, and where the physics of confinement will dominate. It will also allow us to evaluate where resonances give important contributions to the first moment ^{11,12}, as well as to the higher x -moments of the spin structure function $g_1(x, Q^2)$. The moments need to be determined experimentally and calculated in QCD. The well known ‘‘duality’’ between the deep inelastic regime, and the resonance regime observed for the unpolarized structure function $F_1(x, Q^2)$, needs to be explored for the spin structure function $g_1(x, Q^2)$. This will shed new light on this phenomenon. The first round of experiments has been completed on polarized hydrogen (NH_3), deuterium (ND_3), and on 3He . On the theoretical side we now see the first full (unquenched) QCD calculations for the electromagnetic transition from the ground state nucleon to the $\Delta(1232)$ ⁹. Results for other states, and coverage of a larger Q^2 range may soon be available. This may provide the basis for a future QCD description of the helicity structure of prominent resonance transitions.

2. Expectations for $\Gamma_1(Q^2)$

The inclusive doubly polarized cross section can be written as:

$$\frac{1}{\Gamma_T} \frac{d\sigma}{d\Omega dE'} = \sigma_T + \epsilon\sigma_L + P_e P_t [\sqrt{1 - \epsilon^2} A_1 \sigma_T \cos \psi + \sqrt{2\epsilon(1 + \epsilon)} A_2 \sigma_T \sin \psi] \quad (3)$$

where A_1 and A_2 are the spin-dependent asymmetries, ψ is the angle between the nucleon polarization vector and the \vec{q} vector, ϵ the polarization parameter of the virtual photon, and σ_T and σ_L are the total absorption cross sections for transverse and longitudinal virtual photons. For electrons and nucleons polarized along the

beam line, the experimental double polarization asymmetry is given by

$$A_{exp} = P_e P_t D \frac{A_1 + \eta A_2}{1 + \epsilon R} \quad (4)$$

where D and η are kinematic factors, ϵ describes the polarization of the virtual photon, and $R = \sigma_L/\sigma_T$. The asymmetries A_1 and A_2 are related to the spin structure function g_1 by

$$g_1(x, Q^2) = \frac{\tau}{1 + \tau} [A_1 + \frac{1}{\sqrt{\tau}} A_2] F_1(x, Q^2) \quad (5)$$

where F_1 is the unpolarized structure function, and $\tau = \nu^2/Q^2$.

The GDH and Bjorken sum rules provide constraints at the kinematic endpoints $Q^2 = 0$ and $Q^2 \rightarrow \infty$. The evolution of the Bjorken sum rule to finite values of Q^2 using pQCD and the twist expansion allow to connect experimental values measured at finite Q^2 to the endpoints. Heavy Baryon Chiral Perturbation Theory (HBChPT) has been proposed as a tool to evolve the GDH sum rule to $Q^2 > 0$, possibly to $Q^2 = 0.1 \text{ GeV}^2$, and to use the twist expansion down to $Q^2 = 0.5 \text{ GeV}^2$ ⁸. If this is a realistic concept, and if lattice QCD can be used to describe prominent resonance contributions to $\Gamma_1(Q^2)$ in the range $Q^2 = 0.1 - 0.5 \text{ GeV}^2$, *this could provide the basis for a description of a basic quantity of nucleon structure physics from small to large distances within fundamental theory*, a worthwhile goal!

Using the constraints given by the two endpoint sum rules we may already get a qualitative picture of $\Gamma_1^p(Q^2)$ and $\Gamma_1^n(Q^2)$. There is no sum rule for the proton and neutron separately that has been verified. However, experiments have determined the asymptotic limit with sufficient confidence for the proton and the neutron. At large Q^2 , Γ_1 is expected to approach this limit following the pQCD evolution from finite values of Q^2 . At small Q^2 , Γ_1 must approach zero with a slope given by (2).

Heavy Baryon ChPT in the lowest non trivial order predicts¹⁸

$$2M_p^2 \Gamma_1^p(Q^2) = -\frac{\kappa_p^2}{4} Q^2 + 6.85 Q^4 (\text{GeV}^2) + \dots \quad (6)$$

$$2M_n^2 \Gamma_1^n(Q^2) = -\frac{\kappa_n^2}{4} Q^2 + 5.54 Q^4 (\text{GeV}^2) + \dots \quad (7)$$

Unfortunately, the large coefficients of the Q^4 terms make the convergence of this expansion unlikely for $Q^2 > 0.1 \text{ GeV}^2$. However, for the proton-neutron difference the situation is quite different¹⁹

$$2M^2 \Gamma_1^{(p-n)}(Q^2) = -\frac{\kappa_p^2 - \kappa_n^2}{4} Q^2 + 1.31 Q^4 (\text{GeV}^2) + \dots \quad (8)$$

The Q^4 coefficient is a factor 4-5 smaller than for the proton or neutron, and one might expect convergence up to considerably higher Q^2 than for proton and neutron separately. This may be due to the absence of the $\Delta(1232)$ in $\Gamma_1^{(p-n)}$, and may hint at difficulties in describing the $\Delta(1232)$ contributions in HBChPT.

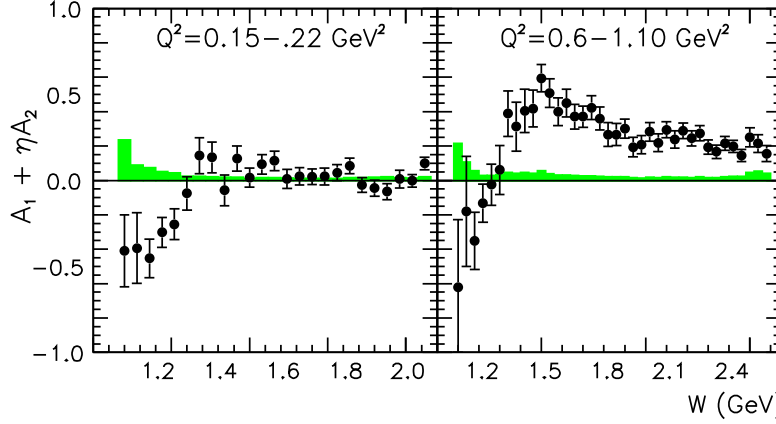


Figure 1: Asymmetry $A_1 + \eta A_2$ for protons. The panels show results for two Q^2 values measured at 2.6 and 4.3 GeV beam energies.

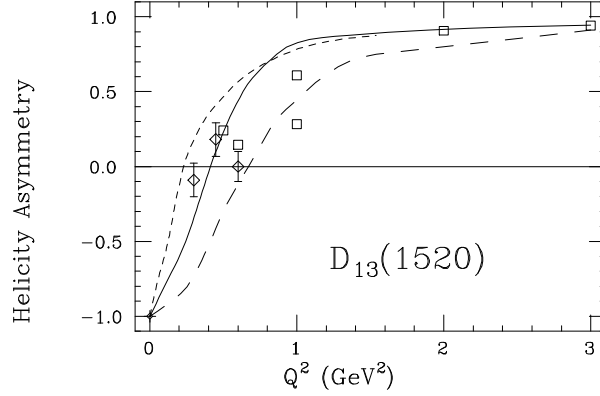


Figure 2: Helicity asymmetry $A_1(Q^2)$ for the $D_{13}(1520)$ resonance transition. A_1 has been extracted from partial wave analyses of single pion electroproduction data.

3. Results for Protons and Neutrons.

Inclusive double polarization experiments have been carried out for energies of 2.6 and 4.3 GeV using $N\vec{H}_3$ ²¹ as polarized hydrogen target with CLAS. After subtracting the nuclear background measured in separate data runs, and using a parameterization of previous unpolarized measurements for R , equation (4) is used to determine the asymmetry $A_1 + \eta A_1$. More details of the analysis can be found in ref.¹³. Two of several Q^2 bins are shown in Figure 1. In the lowest Q^2 bin, the asymmetry is dominated by the excitation of the $\Delta(1232)$ giving a significant negative contribution to A_1 . At higher Q^2 the asymmetry in the $\Delta(1232)$ region remains negative, but at higher W the asymmetry quickly becomes positive and large, reaching peak values of about 0.6 at $Q^2 = 0.8 \text{ GeV}^2$ and $W=1.5 \text{ GeV}$. Evaluations of resonance contributions show that this is largely driven by the $S_{11}(1535)$ $A_{1/2}$

amplitude, and by the rapidly changing helicity structure of the $D_{13}(1520)$ state. The latter resonance is known to have a dominant $A_{3/2}$ amplitude at the photon point, but is rapidly changing to $A_{1/2}$ dominance for $Q^2 > 0.5 \text{ GeV}^2$. The helicity asymmetry $A_1(D_{13}(1520))$ is shown in Figure 2.

Using a parameterization of the world data on $F_1(x, Q^2)$ and $A_2(x, Q^2)$, we can extract $g_1(x, Q^2)$ from (5). Results are shown in Figure 3. The main feature at low Q^2 is due to the negative contribution of the $\Delta(1232)$ resonance. With increasing Q^2 , however, the absolute strength of the $\Delta(1232)$ contribution decreases, while contributions of higher mass resonances increase and become more positive. Note, that higher mass contributions at fixed Q^2 appear at lower x in this graph. The graphs also show a model parameterization of $g_1(x, Q^2)$ which is used to extrapolate to $x \rightarrow 0$. The model is based on a parametrization of the resonance transition formfactors and also describes the behavior of the spin structure functions in the deep inelastic regime.

3.1. *Is Quark-Hadron Duality valid for g_1 of the Proton?*

More than 3 decades ago, Bloom and Gilman¹⁴ found that parametrizations of inclusive unpolarized structure functions, measured in the deeply inelastic regime, approximately describe the resonance region provided one averages over the resonance bumps. This phenomenon is known as local duality. By comparing g_1 at various Q^2 we can infer if such a behavior is also observed for the polarized structure function. For the relatively low Q^2 measured in this experiment the Nachtmann variable $\xi = 2x/(1 + \sqrt{1 + 4x^2m^2/Q^2})$, which accounts for target mass effects, is a more appropriate scaling variable than the Bjorken variable x . Figure 4 shows $g_1(\xi, Q^2)$ for the proton in comparison with the scaling curve describing the deeply inelastic behavior.

The negative contribution of the $\Delta(1232)$ obviously prevents a naive “local duality” to work for $Q^2 < 1.1 \text{ GeV}^2$. Recently, Close and Isgur discussed in a simple harmonic oscillator model¹⁵ that local duality is expected to work only if one integrates over states belonging to certain multiplets within the $SU(6)$ symmetry group. In this case, for local duality to work for the $\Delta(1232)$, one would also need to include contributions from the proton ground state, which belongs to the same multiplet $[56, 0^+]$ as the $\Delta(1232)$. The positive contribution of elastic scattering to g_1 could therefore offset the negative Δ contribution. Detailed duality tests for the higher mass resonances will require a separation of overlapping states belonging to the same multiplet, and measurement of their transition amplitudes. Such a program is currently underway at JLab¹⁶.

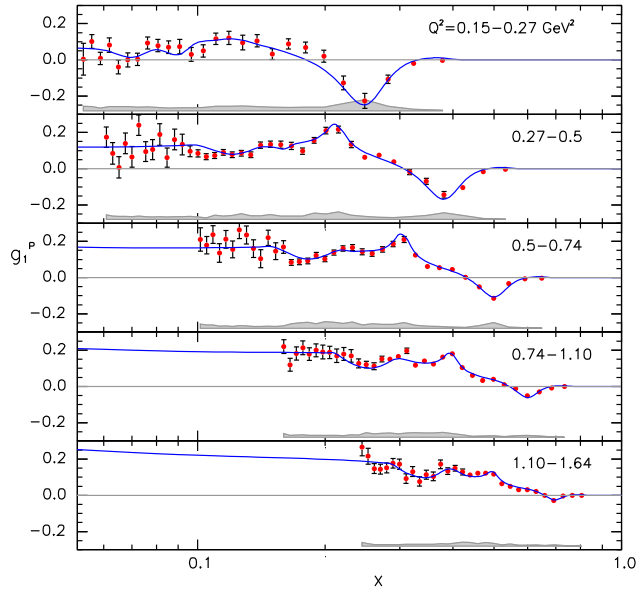


Figure 3: Spin structure function $g_1(x, Q^2)$ for the proton. The curve is a parameterization tuned to fit the JLab data, and is linked to the deep inelastic region based on prior knowledge. It is used for radiative corrections, and to extrapolate g_1 to $x = 0$ for evaluation of Γ_1 .

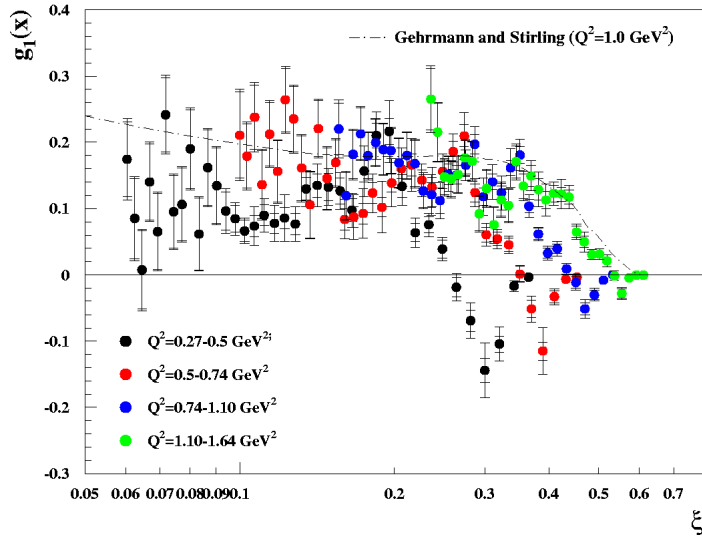


Figure 4: Duality test for g_1 on the proton. The Nachtmann scaling variable ξ is used to account for target mass effects.

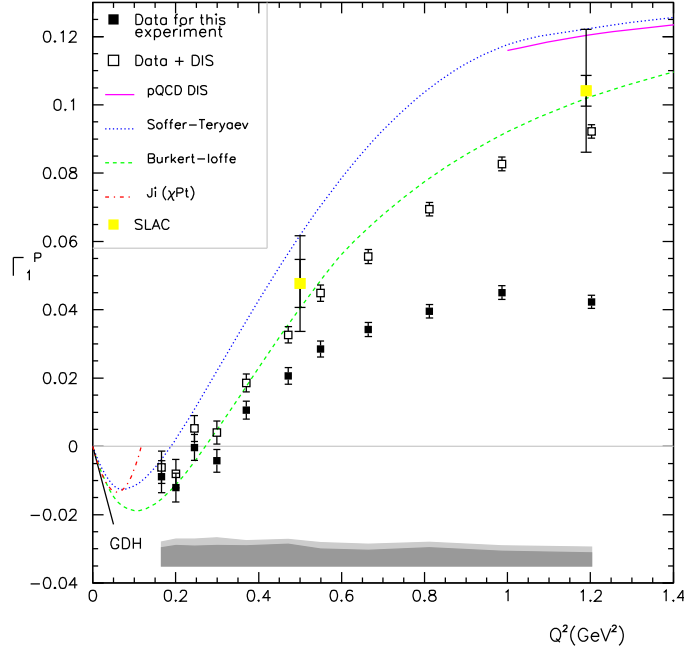


Figure 5: First moment $\Gamma_1(Q^2)$ for the proton. The black symbols correspond to the measured values from CLAS. The open squares are CLAS data corrected for the DIS contributions. Data from SLAC are shown for comparison.

4. The First Moment of Structure Function g_1

In order to obtain the first moment, the integral $\int_0^1 g_1(x, Q^2) dx$ is computed using the measured data points and the parameterization to extrapolate to $x = 0$. The elastic contribution has not been excluded in the integral. The results for $\Gamma_1^p(Q^2)$ of the proton are shown in Figure 5. The characteristic feature is the strong Q^2 dependence for $Q^2 < 1 \text{ GeV}^2$, with a zero crossing near $Q^2 = 0.25 \text{ GeV}^2$. The zero crossing is largely due to an interplay between the excitation strength of the $\Delta(1232)$ and the $S_{11}(1535)$, and the rapid change in the helicity structure of the $D_{13}(1520)$ from helicity $\frac{3}{2}$ dominance at the real photon point to helicity $\frac{1}{2}$ dominance at $Q^2 > 0.5 \text{ GeV}^2$. The latter behavior is well understood in dynamical quark models²⁰. A similar helicity flip is also observed for the $F_{15}(1680)$.

Measurements on ND_3 have been carried out in CLAS²², and on ^3He in Hall A²⁵ to measure the corresponding integrals for the neutron. Here I only discuss the Hall A results. Data were taken with the JLab Hall A spectrometers using a polarized ^3He target. Since the data were taken at fixed scattering angle, Q^2 and ν are correlated. Cross sections at fixed Q^2 are determined by an interpolation between measurements at different beam energies. Both longitudinal and transverse settings of the target polarization were used. After correcting for nuclear effects and accounting for the deep inelastic part of the integral, the first moment of $g_1(x, Q^2)$ for neutrons can be extracted, and is shown in Figure 6. The data deviate from

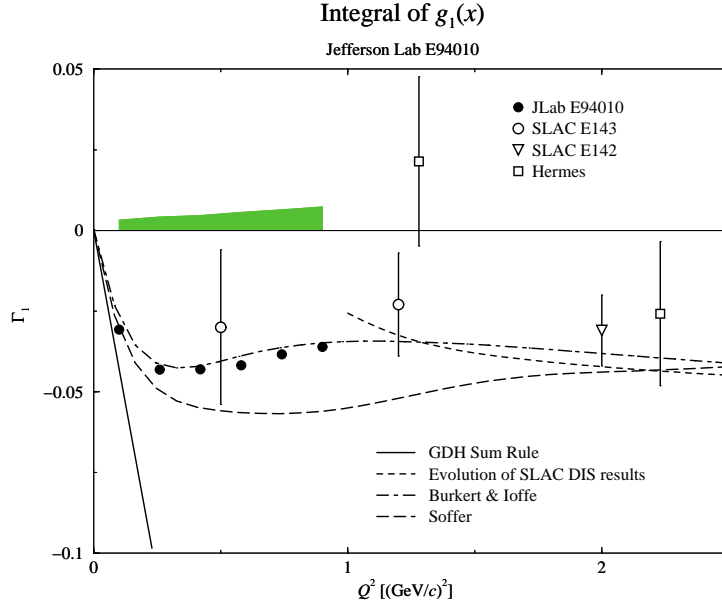


Figure 6: Preliminary results of the first moment of spin structure function g_1 for neutrons, corrected for the unmeasured deep inelastic part. The band indicates the size of systematic errors.

the trend seen for the pQCD-evolved asymptotic behavior for $Q^2 < 1 \text{ GeV}^2$. This is largely due to the contribution of the $\Delta(1232)$. The data are well described by a model¹² that includes resonance excitations and describes the connection to the deep inelastic regime assuming vector meson dominance. Another parametrization of the Q^2 dependence is from Soffer and Teryaev²⁶.

5. The Bjorken Integral

Using the results on $\Gamma_1(Q^2)$ for protons and neutrons one can determine the Q^2 dependence of the Bjorken integral $\Gamma_1^{(p-n)} = \Gamma_1^p - \Gamma_1^n$. In this integral, all contributions of isospin $\frac{3}{2}$ resonances, such as the $\Delta(1232)$, drop out, and contributions of other resonances may be reduced as well. Also, since the GDH sum rule for the proton-neutron difference is positive, no zero-crossing is necessary to connect to the asymptotic behavior. The preliminary data are shown in Figure 7. Since the CLAS data and the Hall A data were measured at somewhat different Q^2 values, the data in each set were connected with a smooth interpolating curve and then subtracted. The resulting curve is the centroid of the shaded error band. The band at higher Q^2 corresponds to the $O(\alpha_s^3)$ evolution of the Bjorken sum rule. At low Q^2 the HBChPT curve seems to describe the trend of the data up to $Q^2 \approx 0.2 \text{ GeV}^2$. A recent ChPT calculation²⁷ in $O(p^4)$ predicts values significantly above the HBChPT

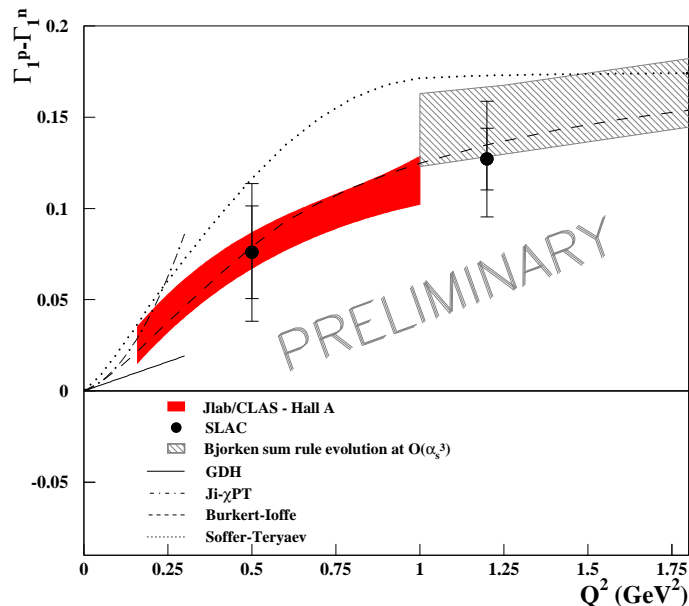


Figure 7: Preliminary results for the Bjorken integral of the proton-neutron difference. The band below $Q^2 = 1 \text{ GeV}^2$ parametrizes the data and error for both data sets.

curve. The model with explicit resonance contributions gives a good description of the global behavior for both proton and neutron targets, and for their difference.

6. Conclusions

First high precision measurements of double polarization responses have been carried out at Jefferson Lab in a range of Q^2 not covered in previous high energy experiments. Spin structure functions and spin integrals $\Gamma_1(Q^2)$ have been extracted for protons and neutrons. The proton and neutron data both show large contributions from resonance excitations. $\Gamma_1^p(Q^2)$ shows a dramatic change with Q^2 , including a sign change near $Q^2 = 0.25 \text{ GeV}^2$, while $\Gamma_1^n(Q^2)$ remains negative, however is strongly affected by the $\Delta(1232)$ contribution. Qualitatively, the strong deviations from the trend of the deep inelastic behavior for $Q^2 < 1 \text{ GeV}^2$ mark the transition from the domain of single and multiple parton physics to the domain of resonance excitations and hadronic degrees of freedom.

New data have been taken both on hydrogen and deuterium with nearly 10 times more statistics, and higher target polarizations, and cover a larger range of energies from 1.6 GeV to 5.75 GeV. The year 2001 data cover a Q^2 range from 0.05 to 3 GeV^2 , and a larger part of the deep inelastic regime than the data presented here. This will allow a reduction of the systematic uncertainties related to the extrapolation to $x = 0$. Moreover, since data are available at fixed Q^2 taken at different beam energies, a separation of $A_1(Q^2, W)$ and $A_2(Q^2, W)$ will be possible. The new

data will also give much better sensitivity to resonance production in exclusive channels, such as $ep \rightarrow en\pi^+$, that have been measured previously²³. Finally, at the higher energies, CLAS will be able to study single and double spin asymmetries in various exclusive and semi-inclusive reactions currently of great interest to access the transverse quark distribution functions²⁴.

There is a program underway in JLab Hall A to measure the GDH integral for neutrons down to extremely small Q^2 values²⁸, near the real photon point, and to measure the asymmetry $A_1(x, Q^2)$ for the neutron at high x ²⁹. High precision data for A_1 and A_2 at $Q^2 = 1 \text{ GeV}^2$ are also expected to come from experiment E-01-006 in Hall C³⁰.

The Southeastern University Research Association (SURA) operates JLab for the U.S. Department of Energy under Contract No. DE-AC05-84ER40150.

1. J. Ashman et al., Nucl. Phys. B328, 1 (1989)
2. for a recent overview see: B. Filipone and X. Ji, Adv. Nucl. Phys. 26, 1 (2001).
3. J.D. Bjorken, Phys. Rev. 179, 1547 (1969)
4. S.B. Gerasimov; Sov. J. Nucl. Phys. 2, 430 (1966).
5. S.D. Drell and A.C. Hearn, Phys. Rev. Lett.16, 908 (1966).
6. J. Ahrens et al., Phys.Rev.Lett.87:022003 (2001); also: talk at GDH2002.
7. X. Ji, J. Osborne, J. Phys. G27 127 (2001).
8. X. Ji, in: Excited Nucleons and Hadronic Structure, World Scientific (2001)
9. C. Alexandrou et al., hep-lat/0209074 (2002).
10. K. Abe et al., Phys. Rev. D58, 2003 (1998).
11. V. Burkert and Zh. Li, Phys. Rev. D47, 46 (1993).
12. V. Burkert, B. Ioffe, Phys. Lett. B296, 223 (1992); J. Exp. Theo. Phys.78, 619(1994).
13. R. Minehart, in: NSTAR2001, World Scientific, eds. D. Drechsel, L. Tiator (2001)
14. E.D. Bloom and F.G. Gilman, Phys. Rev. Lett. 25, 1140 (1970)
15. F.E. Close and N. Isgur, Phys. Lett. B509, 81 (2001)
16. For a recent overview see: V.D. Burkert, hep-ph/0210321
17. J. Soffer and O. Teryaev, Phys. Rev. D51, 25 (1993)
18. X. Ji, C.W. Kao, J. Osborne, Phys.Lett.B472:1-4 (2000)
19. V. Burkert, Phys. Rev. D63, 97904 (2001)
20. F. E. Close and F.J. Gilman, Phys. Letts. 38B, 541 (1972).
21. V. Burkert, D. Crabb, R. Minehart, et al., JLab experiment E-91-023.
22. S. Kuhn, G. Dodge, M. Taiuti, et al., JLab experiment E-93-009.
23. R. De Vita et al., Phys. Rev. Letts. 88, 082001-1 (2002).
24. H. Avakian, talk at SPIN2002, to be published in the proceedings.
25. G. Cates, J.P. Chen, Z.E. Meziani et al., JLab experiment E-94-010.
26. J. Soffer and O.V. Teryaev, Phys. Rev.D56, 7458 (1997).
27. V. Bernard, T. Hemmert, and U. Meissner, Phys. Lett. B545, 105-111, (2002).
28. J.P. Chen, A. Deur, and F. Garibaldi, et al., Jlab Experiment E-97-110.
29. J.P. Chen, Z.E. Meziani, P. Souder, et al., Jlab Experiment E-99-117.
30. O. Rondon, et al., Experiment E-01-006 (2001).